Talanta 232 (2021) 122386

Contents lists available at ScienceDirect

Talanta

journal homepage: www.elsevier.com/locate/talanta

Pyrroloquinoline quinone-dependent glucose dehydrogenase bioelectrodes based on one-step electrochemical entrapment over single-wall carbon nanotubes

Andrés Felipe Quintero-Jaime [a], Felipe Conzuelo [c,**], Diego Cazorla-Amorós [b], Emilia Morallón [a,*]

[a] Departamento de Química Física and Instituto Universitario de Materiales de Alicante (IUMA), University of Alicante, Ap. 99, 03080, Alicante, Spain
[b] Departamento de Química Inorgánica and Instituto Universitario de Materiales de Alicante (IUMA), University of Alicante, Ap. 99, 03080, Alicante, Spain
[c] Analytical Chemistry – Center for Electrochemical Sciences, Faculty of Chemistry and Biochemistry, Ruhr University Bochum, Universitätsst. 150, D-44780, Bochum, Germany

ARTICLE INFO

Keywords:
Entrapment
Carbon nanotubes
Phosphonic acid
PQQ-GDH
Biosensor
Glucose

ABSTRACT

Development of effective direct electron transfer is considered an interesting platform to obtain high performance bioelectrodes. Therefore, designing of scalable and cost-effective immobilization routes that promotes correct direct electrical contacting between the electrode material and the redox enzyme is still required. As we present here, electrochemical entrapment of pyrroloquinoline quinone-dependent glucose dehydrogenase (PQQ-GDH) on single-wall carbon nanotube (SWCNT)-modified electrodes was carried out in a single step during electrooxidation of *para*-aminophenyl phosphonic acid (4-APPA) to obtain active bioelectrodes. The adequate interaction between SWCNTs and the enzyme can be achieved by making use of phosphorus groups introduced during the electrochemical co-deposition of films, improving the electrocatalytic activity towards glucose oxidation. Two different procedures were investigated for electrode fabrication, namely the entrapment of reconstituted holoenzyme (PQQ-GDH) and the entrapment of apoenzyme (apo-GDH) followed by subsequent *in situ* reconstitution with the redox cofactor PQQ. In both cases, PQQ-GDH preserves its electrocatalytic activity towards glucose oxidation. Moreover, in comparison with a conventional drop-casting method, an important enhancement in sensitivity was obtained for glucose oxidation (981.7 ± 3.5 nA mM^{-1}) using substantially lower amounts of enzyme and cofactor (PQQ). The single step electrochemical entrapment in presence of 4-APPA provides a simple method for the fabrication of enzymatic bioelectrodes.

1. Introduction

The design of enzymatic bioelectrodes has received great attention as a fundamental part in technologies for green-energy production based on electrochemical biofuel cells (EBFC), food chemistry and biosensing [1–3]. In this sense, the current research has mainly focused in the development of scalable, controlled and reproducible procedures for the synthesis of biologically modified surfaces, which can provide active bioelectrodes with efficient electron-transfer (ET) between the enzyme and the electrode, as well as high sensitivity and stability [4–6]. Among the possible alternatives, the development of architectures providing direct electron transfer (DET) between the biocatalyst (i.e., enzyme) and the electrode surface is considered as a promising way to ensure high turnover rates of the redox enzyme and high kinetics rates of the ET process [7,8]; while at the same time avoiding the use of external redox mediators (e.g., NAD^+). Unfortunately, acquiring bioelectrodes based on DET mechanism is still challenging in the designing of bioelectrochemical devices, mostly by the hindered effect of the glycosylation shell of the enzyme that can bury the redox cofactor, affecting the efficient electron transfer [9–11]. Therefore, great efforts in current research have been addressed in obtain electrical contacting of redox enzyme with the electrode surface able of providing a DET mechanism [12,13].

Here lies the importance of development of immobilization methods

* Corresponding authors.
** Corresponding author.
E-mail address: morallon@ua.es (E. Morallón).

https://doi.org/10.1016/j.talanta.2021.122386
Received 4 March 2021; Received in revised form 29 March 2021; Accepted 30 March 2021
Available online 16 April 2021

during the synthesis of the bioelectrode, in which the appropriate assembling of confined enzymatic element without affecting its catalytic activity is of great relevance [14,15]. Besides, orientation and even interconnection of the redox cofactor with the electrode surface can provide platforms for fast and efficient electron transfer [16,17] by an electron-hopping mechanism [5,18,19] or direct electron transfer [20,21], which confers high efficiency and performance of the bioelectrode.

Despite the wide variety of immobilization procedures, like covalent linkage, adsorption, electrostatic interaction and crosslinking, the confining of the enzyme into an inorganic (i.e. sol-gel) or polymeric matrix provides an interesting route to generate a close interaction between the electrode and the enzyme [11,22,23]. Additionally, entrapment assisted by electrochemical methods affords an easy, scalable and controlled preparation of the bioelectrode [14,24–26]. The entrapment based on the electrochemical deposition of a polymer with other components like chitosan is considered as a simple, fast, uniform and controllable immobilization route [27,28]. However, in these examples, the polymers have low conductivity and lack of electroactivity, what makes that the mediation of electron transfer is impeded. However, the entrapment in redox active polymers based on osmium complexes or its copolymers with non-electroactive polymers have demonstrated outstanding performance not only in the proper immobilization of the enzymatic element, but also in the improvement of the electron transfer [16,18,29]. Moreover, other redox species like ferrocene-derivatives, methyl viologen or Ru-complexes have also been employed with remarkable results [30–32].

Conjugated polymers, such as polyaniline (PANI), polypyrrole (Py) and poly(3–4 ethylenedioxythiophene) (PEDOT), can offer a good platform as matrix for electrochemical enzyme entrapment, especially considering the easy and well-known polymerization mechanism and remarkable conductivity [33–36]. Moreover, the incorporation of redox species and the use of substituents in the monomer precursor have improved the redox behavior of the polymer, generating electrochemical functional groups which facilitates the electron transfer [36,37].

In the present work, nitrogen and phosphorus functionalities electrochemically incorporated on SWCNTs have been employed as suitable building-blocks to develop efficient direct electron transfer-based bioelectrodes in a single step, using low amounts of enzyme. Here two different routes for the fabrication of bioelectrodes have been studied, employing previously reconstituted PQQ-GDH, as well as the possibility for integration of apo-GDH that can be reconstituted *in situ* after electrode preparation. In these routes, electrochemical entrapment of PQQ-GDH can be done during oxidation of 4-APPA at different upper limit potentials that incorporate N and P functionalities on single-wall carbon nanotubes modified electrodes, maintaining the catalytic activity of the redox enzyme. Interestingly, the degree of functionalization and electrocatalytic performance of the bioelectrode towards glucose oxidation highly depends on the upper potential limit used during electrochemical entrapment of the enzyme.

2. Experimental section

2.1. Reagents and equipment

Single-wall carbon nanotubes (SWCNTs) with purity 99% (1–4 nm diameter, 3–30 μm length) were purchased from Cheap Tubes Inc. (Cambridgeport, USA). The specific surface area, obtained by the Brunauer-Emmett-Teller (BET) method, was 587 $m^2\ g^{-1}$.

Soluble apoenzyme glucose dehydrogenase (apo-GDH) was obtained from Roche Diagnostics (Germany). 4-Aminophenyl phosphonic acid (4-APPA, +98%) used as modifier agent was purchased from Tokyo Chemical Industry (TCI-Belgium). Potassium dihydrogen phosphate (KH_2PO_4) and dipotassium hydrogen phosphate trihydrate ($K_2HPO_4{\cdot}3H_2O$) were purchased from VWR Chemicals, and used to prepare the phosphate buffer solution (0.1 M PBS, pH = 7.2). 4-(2-Hydroxyethyl)-1-piperazineethanesulfonic acid (HEPES) (≥99.5%-titration), D-(+)-glucose (ACS reagent), pyrroloquinoline quinone (PQQ, ≥95%-HPLC) and dimethylformamide (DMF) were purchased from Sigma-Aldrich. All the solutions were prepared using ultrapure water (18 MΩ cm, SG water). Ar (99.999%) was provided by Air Liquide.

2.2. Electrochemical entrapment of enzyme

2.2.1. Enzymatic electrolyte solutions

Firstly, an aqueous solution containing 10 mM HEPES, 150 mM $CaCl_2$, 0.1 M KCl and 1 mM 4-APPA was prepared to attain a buffer solution with pH = 5.0. This solution is named as HEPES electrolyte, which have been employed for the electrochemical entrapment. Depending on the synthesis procedure (Scheme 1), the model enzyme (glucose dehydrogenase) can be incorporated into the buffer solution in different ways as follows:

Solution for holoenzyme entrapment: Firstly, reconstitution of the s-GDH was carried out with PQQ following the next steps. Step 1, 36 mg of apo-GDH were dissolved in a freshly prepared buffer solution (pH = 7.0), containing 10 mM HEPES, 150 mM $CaCl_2$ and 520 μM PQQ (solution 1 in Scheme 1), in order to attain a concentration of 36 mg mL^{-1}. This enzymatic solution was mixed at 1600 rpm for 30 min in vortex and stored at 4 °C until its use. In this procedure, PQQ cofactor is introduced in the apo-GDH structure as active center and the complex is stabilized by the presence of three calcium cations [38]. Step 2, in order to avoid further mediating effects of free PQQ which can be adsorbed onto the electrode surface, a purification process was carried out. The 36 mg mL^{-1} solution of PQQ-GDH was treated in a centrifugal concentrator Eppendorf (VIVASPIN 500) with a membrane cut-off of 10 kDa. Centrifugation was carried out at 6000 rpm during 25 min, separating the reconstituted enzyme and free-PQQ in excess, latest one discarded. Step 3, an aliquot of this enzymatic PQQ-GDH solution was added to the HEPES electrolyte to attain a final concentration of 5 mg mL^{-1} PQQ-GDH. All the enzyme solutions were stored at 4 °C until used (see Scheme 1-Procedure 1).

Solution for apo-GDH entrapment: In this part only the apo-GDH was dissolved in the HEPES electrolyte until a concentration of 5 mg mL^{-1} was obtained (see Scheme 1-Procedure 2).

2.2.2. One-step electrochemical synthesis of bioelectrodes

The working electrode for the electrochemical modification was prepared using a glassy carbon rod (GC) as support, modified with SWCNTs. 1 mg of SWCNTs was dispersed in DMF employing an ultrasonic cold-bath for 45 min, achieving a dispersion of 1 mg mL^{-1} SWCNTs. Prior to the deposition of SWCNTs, the glassy carbon electrode surface (3 mm diameter) was sanded with emery paper and polished using 1 μm and 0.05 μm alumina slurries, then rinsed with ultrapure water in an ultrasonic bath. Afterwards, a 5 μL aliquot of the dispersion was dropped onto the glassy carbon surface and dried under an infrared lamp to remove the solvent. This procedure was repeated twice, completing 10 μL of the SWCNTs suspension over the GC surface.

Electrochemical entrapment of the enzyme onto the SWCNT modified electrode was performed by cyclic voltammetry, submitting the sample to 50 cycles at 50 mV s^{-1}, at different upper potential limits. The equipment used was an Autolab PGSTAT 302 (Metrohm, the Netherlands) potentiostat station, in which the glassy carbon electrode modified with SWCNTs was the working electrode (WE), a platinum wire was used as counter electrode (CE) and a Ag/AgCl (3 M KCl) introduced in a Luggin capillary, filled with the same electrolyte without 4-APPA and enzyme, was used as reference electrode (RE). The electrolyte employed was a deoxygenated HEPES electrolyte with 5 mg mL^{-1} of the enzyme in both procedures.

Depending on the procedure employed (see Scheme 1), after the electrochemical immobilization, the bioelectrodes were washed with excess of buffer solution (pH = 7.0) to remove excess of electrolyte and weakly adsorbed enzyme. In case of entrapment of the apo-GDH, after

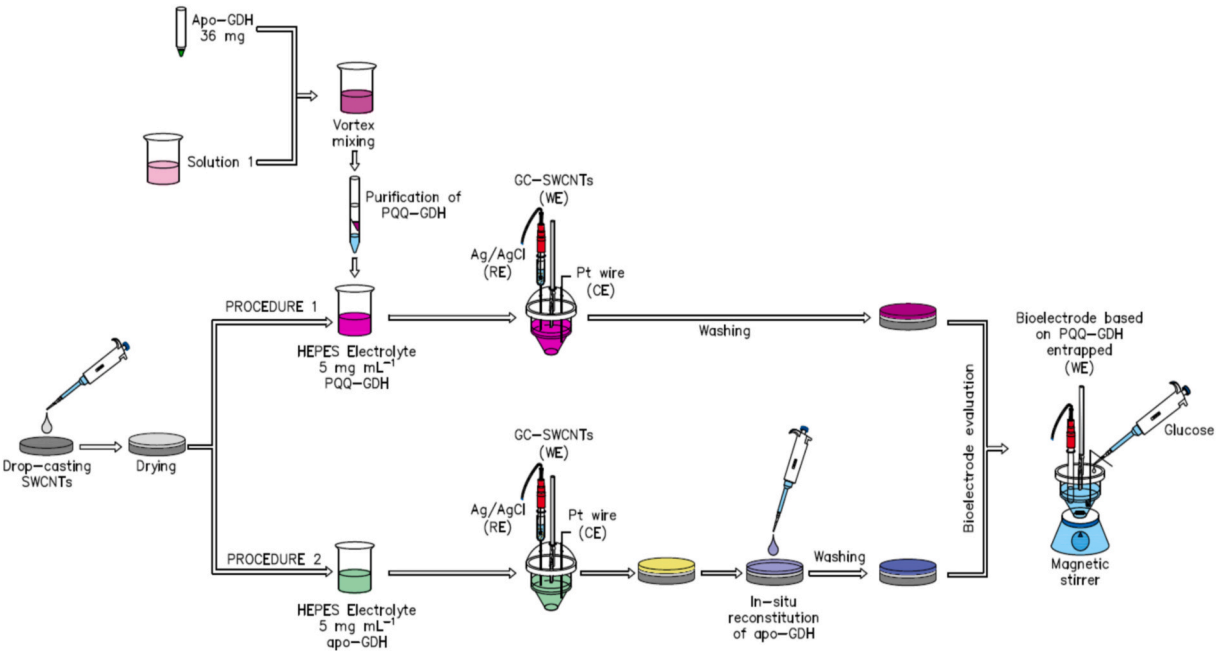

Scheme 1. Single step electrochemical immobilization of GDH on SWCNT modified GC electrodes during 4-APPA oxidation. Two procedures for enzyme immobilization were evaluated, procedure 1: the reconstituted holoenzyme was used for electrode modification, procedure 2: the apo-GDH was first immobilized and reconstituted *in situ*.

electrochemical immobilization an aliquot of 5 μL of a solution of 40 μM PQQ in buffer solution (10 mM HEPES and 150 mM $CaCl_2$, pH = 7.0) was dropped on the electrode and incubated at 4 °C for 30 min [39]. Afterwards, the electrodes were rinsed to remove any excess of unbound PQQ.

For the electrodes prepared with the holoenzyme, they are named as PQQ-GDH@SWCNT-APPA-X. In the case of the apo-GDH entrapment, the electrodes are named as GDH@SWCNT-APPA-X and GDH/PQQ@SWCNT-APPA-X before and after the reconstitution with PQQ, respectively. For electrodes synthesized in the same conditions but without the presence of enzyme the nomenclature employed was SWCNT-APPA-X. In all cases, X represents the upper potential limit that was employed for the electrochemical entrapment.

An additional SWCNT-APPA-1.15 electrode was prepared for comparison purposes in which the reconstituted holoenzyme was immobilized by drop-casting 5 μL of 36 mg mL^{-1} of PQQ-GDH (SWCNT-APPA-X- $PQQ\text{-}GDH_{drop\ casting}$).

The surface concentration of PQQ that is related with the reconstituted enzyme, was determined from the charge of the redox process in the cyclic voltammograms using the following equation (Eq. (1)):

$$\Gamma = \frac{Q}{nFA} \quad \text{(Eq. 1)}$$

Where Γ is the estimated surface concentration of PQQ-GDH (mol cm^{-2}), n is the number of transferred electrons (2 e^-), F is the Faraday constant (96485C mol^{-1}), and A is the active surface area (0.587 cm^2), which was determined using the specific surface area (S_{BET} = 587 m^2 g^{-1}) of the deposited SWCNTs in the same electrolyte. Q is the electrical charge obtained from the integration of the anodic peak associated with the cofactor in the enzyme. The charge contribution of the SWCNT-APPA-X electrode without enzyme was subtracted.

2.3. Physicochemical characterization

X-Ray photoelectron spectroscopy (XPS) was performed in a VG-Microtech Mutilab 3000 spectrometer using Al Kα radiation (1253.6 eV). The deconvolution of the XPS signals for C1s, O2p, P2p and N1s was done by least squares fitting using Gaussian-Lorentzian curves, while a Shirley line was used for the background determination. The P2p spectra have been analyzed considering the spin-orbit splitting into 2p3/2 and 2p1/2 with a 2:1 peak area ratio and 0.87 eV splitting [40].

Scanning electron micrographs were taken using an ORIUS SC600 model Field Emission Scanning Electron Microscope (FE-SEM) and a ZEISS microscope, Merlin VP Compact model. The samples were coated with a thin layer of carbon to avoid decomposition of the enzyme and the different oligomers incorporated by the electrochemical modification of 4-APPA.

Atomic force microscopy (AFM) images were obtained with an atomic force microscope NT-MDT model Ntegra, coupled with a high resolution silicon AFM cantilever (NSG01 type), with a resonant frequency close to 150 kHz. It was employed in semi-contact mode for the measurements of 10 × 10 μm. The scan rate of the cantilever was 0.5 Hz with a resolution of 256 points in the images.

2.4. Electrochemical characterization and catalytic activity towards glucose oxidation

The electrochemical behavior of the fabricated bioelectrodes was evaluated in 0.1 M PBS (pH = 7.2), in presence and absence of glucose, employing a three electrode configuration cell, where the bioelectrodes were the working electrode (WE), a platinum wire was used as counter electrode (CE) and a Ag/AgCl (3 M KCl) electrode was introduced in the electrochemical cell as reference electrode (RE). Characterization was performed at room atmosphere conditions, taking into account the non O_2-dependence of the enzyme.

Electrochemical catalytic behavior towards glucose oxidation was determined by chronoamperometry, in the same electrochemical cell configuration previously mentioned. In a typical measurement, before the addition of glucose, the working electrode is stabilized at 0.35 V in 0.1 M PBS (pH = 7.2) under room atmosphere conditions and, subsequently, aliquots from a 0.1 M glucose solution were added to the electrochemical cell, obtaining glucose concentrations between 5 μM and 10 mM. The time between the addition of different aliquots was established in 5 min, to guarantee a stabilization of the current after

glucose addition. During the chronoamperometry, stirring conditions were maintained during all the experiment. Cyclic voltammetry was measured at the beginning and the end of the chronoamperometry to follow changes in the electrode.

3. Results and discussion

The electrochemical synthesis of bioelectrodes by entrapment of either apo- or holoenzyme PQQ-GDH has been performed employing electrooxidation of 4-APPA by cyclic voltammetry. In this case, the generated oxidation products introduce functionalities at the SWCNT modified surfaces while enabling co-entrapment of the redox enzyme during the oxidative polarization. The process makes possible a single step fabrication of bioelectrodes, promoting an improved electrical communication with the redox enzyme. In comparison, bioelectrodes prepared using pristine SWCNTs modified with PQQ-GDH did not show any noticeable electrochemical activity towards catalytic glucose oxidation (see Fig. S1).

3.1. Immobilization of reconstituted PQQ-GDH

3.1.1. Electrochemical synthesis of PQQ-GDH@SWCNT-APPA-X electrodes

Fig. 1-A, 1-C and 1-E show the cyclic voltammograms of the electrochemical entrapment of reconstituted glucose dehydrogenase (see Scheme 1) at different upper potential limits. Irreversible oxidation of 4-APPA is observed at potentials more positive than 0.69 V vs. Ag/AgCl (3 M KCl), as well as several redox processes at less positive potentials after this first cycle, which intensity increases with cycling. At the same time, the current associated with the oxidation of 4-APPA decreases. This voltammetric behavior is similar to that observed in absence of GDH in the solution (see Fig. S2) and it has been previously observed in precious works developed in acid media [41]. The observed processes were associated to the functionalization of SWCNTs with the species produced during oxidation of 4-APPA. Steady stored charge of these redox processes with cycling and their electroactive behavior shows the good stability of the redox species at this pH conditions. In presence of the holoenzyme no significant changes in the voltammograms and similar redox process are observed, what indicates that the electrochemical functionalization of SWCNTs is also being produced, although there are some differences in the relative intensities of the redox processes.

Fig. 1-B, 1-D and 1-F contain the voltammograms of the PQQ-GDH@SWCNT-APPA-X electrodes in 0.1 M PBS (pH = 7.2). It can be observed in all the cases the presence of a redox process at −0.11 V associated to the PQQ in the enzyme [42,43], which is not observed in the electrodes synthetized at the same conditions in absence of the enzyme (see Fig. S3). This indicates the adequate direct electron transfer between the immobilized enzyme and the electrode. The redox process that appears in all voltammograms at 0.13 V is associated with the redox species of the functionalities produced by oxidation of 4-APPA. In addition, the occurrence of an increased anodic current response at potentials more positive than the PQQ redox wave in the presence of glucose indicates that the entrapped enzyme remains catalytically active after electrochemical synthesis, as it is observed, for example, by electrochemical entrapment at an upper potential limit of 1.15 V (Fig. 1-F). The surface concentration of PQQ for the assembly exhibiting a prominent catalytic activity, PQQ-GDH@SWCNT-APPA-1.15, has been estimated for three independently prepared electrodes as (5.8 ± 0.8) x 10^{-11} mol cm^{-2}.

3.1.2. Physicochemical characterization of PQQ-GDH@SWCNT-APPA-X electrodes

The results of XPS analysis of the bioelectrodes are shown in Table 1. The XPS spectra presented in Fig. S4 for all the samples, show the presence of two N species at around 398.5 eV and 400 eV. The species at 400 eV, which is the one with the highest intensity, can be assigned to the amide species of the peptide chain and the peak at 398.5 eV could be related to imine species [44]. In this case, amount of nitrogen detected is much higher than the observed in SWCNTs functionalized in acid conditions [41], showing the incorporation of the enzyme and the contribution of the nitrogen-containing groups to N1s peak.

Table 1
Quantification of surface species by XPS and distribution of N, O and P contributions for PQQ-GDH@SWCNT-APPA-X synthesized in HEPES electrolyte at different potentials in presence of 5 mg mL^{-1} PQQ-GDH.

Upper potential limit [V vs. Ag/AgCl (3 M KCl)]	O (at %)	N (at %)	P (at %)	% Imines (398.5 eV)	% Amides (400 eV)	C–O–P 133.3 eV	C–P–O 132.6 eV
Pristine	3.1	0.37	0.0	–	–	–	–
0.75	9.9	6.4	1.7	–	100	62	38
0.95	18.6	25.9	0.5	34	66	10	90
1.15	24.1	13.6	3.1	12	88	14	86

In the case of P2p spectra (Fig. S5), two asymmetric doublets appear in all the electrodes. The first one at 132.6 eV, associated with the binding energy of C–P–O species, in agreement with the phosphonic group of the 4-APPA precursor [36], and the second at 133.3 eV related to phosphoric species (C–O–P) generated from the electrochemical oxidation of the phosphonic group at the anodic polarization conditions [41,45]. However, the percentage of these species changes and depends on the potential conditions used (Table 1). Interestingly, when the entrapment is done at an upper potential limit of 0.95 V or 1.15 V, the main contribution is corresponding to the phosphonic species (i.e., C–P–O 2p3/2 peak at 132.5 eV). This result indicates that the presence of enzyme stabilizes the phosphonic group avoiding its oxidation, which might be as a result of the interaction between this group and the enzyme.

Fig. 2 shows the morphology of the PQQ-GDH@SWCNT-APPA-X electrodes synthesized at the different upper potential limits. Once electrochemical entrapment is performed, the surface of the SWCNTs is covered by a smooth and globular coating, which morphology and thickness depends on the upper potential limit employed during the entrapment. In case of PQQ-GDH@SWCNT-APPA-0.75 (Fig. 2-B) the appearance of isolated enzymatic/APPA deposits can be observed between the interconnected bundles of the SWCNTs. When the upper potential limit increases, the amount of deposit, distribution and thickness increase and the formation of a smooth surface can be observed (Fig. 2-C to 2-F). The morphology is different in comparison to the electrodes prepared in absence of enzyme (see Fig. S6 for pristine SWCNT and SWCNT-APPA-1.15). The morphology of this electrode shows that during the electrochemical functionalization, products generated by the electrooxidation of 4-APPA cover homogeneously the surface of the SWCNTs (see Figs. S6-C and S6-D). The formation of the enzymatic/APPA deposit on the electrode surface is the responsible for the strong changes in morphology observed. The presence of the enzyme during the electrochemical entrapment generates a globular-like structure that makes smoother the surface as observed by AFM microscopy (Fig. S7).

3.1.3. Glucose oxidation on PQQ-GDH@SWCNT-APPA-X electrodes

Fig. 3-A shows the cyclic voltammogram of this bioelectrode in 0.1 M PBS (pH = 7.2) in absence and presence of glucose for the electrodes prepared at an upper potential limit of 1.15 V. Other upper potential limits used during electrode synthesis (0.75 V and 0.95 V) demonstrated an unstable behavior during the electrocatalytic activity towards glucose oxidation, as well as saturation at low concentrations of glucose. Therefore, a study of the response towards glucose oxidation using those electrodes was discarded. In presence of glucose, the contribution in the oxidation current is 471.23 nA at 0.4 V for the PQQ-GDH@SWCNT-APPA-1.15 electrode.

Chronoamperometry response of the PQQ-GDH@SWCNT-APPA-

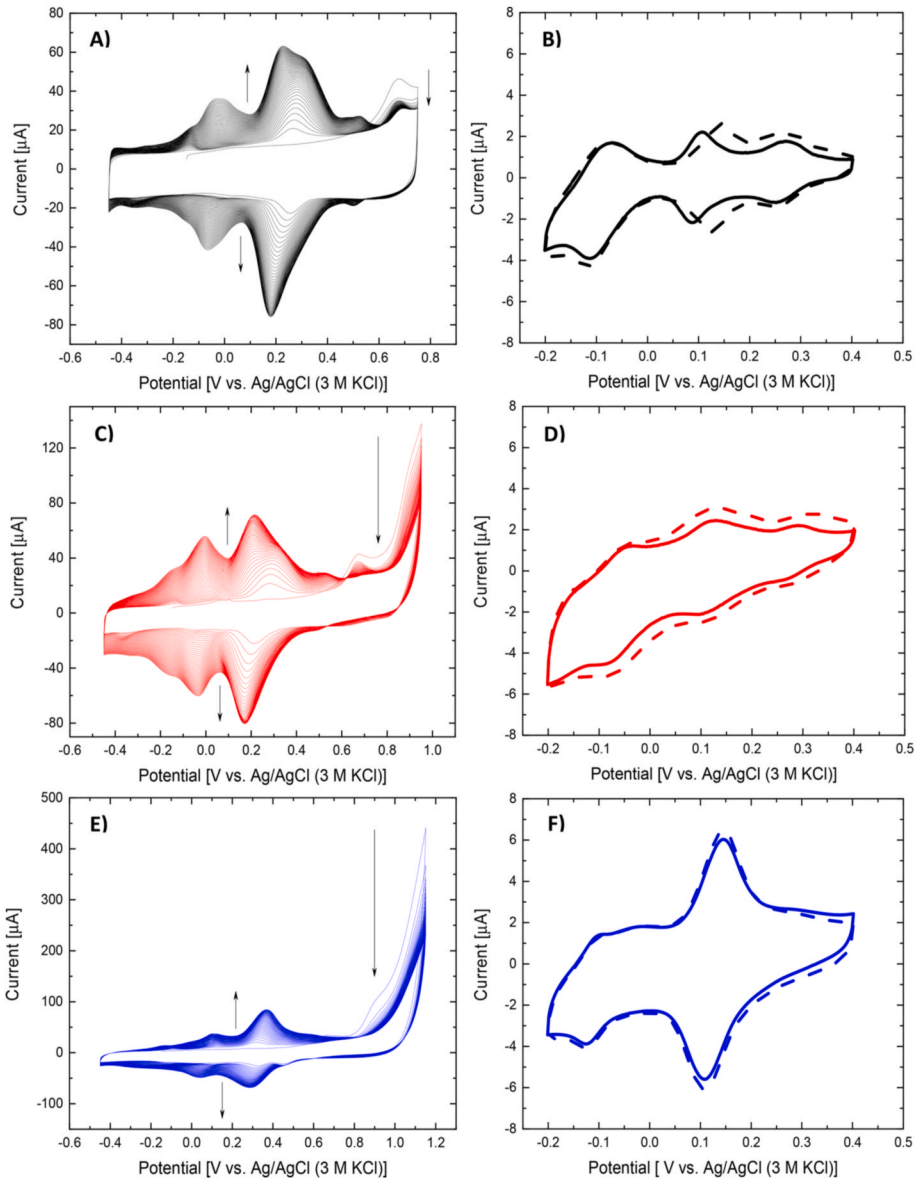

Fig. 1. Cyclic voltammograms during electrochemical entrapment of purified PQQ-GDH solution on SWCNTs at different upper potential limit in HEPES electrolyte + 5 mg mL^{-1} PQQ-GDH (pH = 5.0) at 50 mV s^{-1} for 50 cycles under Ar atmosphere: A) 0.75 V, C) 0.95 V and E) 1.15 V. Electrochemical characterization by cyclic voltammetry of PQQ-GDH@SWCNT-APPA-X in absence (dashed line) and presence (solid line) of 4 mM of glucose in 0.1 M PBS (pH = 7.2) under room atmosphere conditions at 5 mV s^{-1}, for electrodes prepared at upper potential limits being: B) 0.75 V, D) 0.95 V and F) 1.15 V.

1.15 electrode (Fig. 3-B) shows an increase in the oxidation current after each addition of glucose. The variation of the current referred to the enzyme concentration versus the glucose concentration presents a typical Michaelis-Menten behavior. The Lineweaver-Burk fitting allowed to determine a value of K_m^{app} of 0.19 mM (see inset in Fig. 3-C), which is lower than those reported previously for other biosensors [46, 47]. The low value of K_m^{app} obtained suggests a high affinity between the enzyme and the substrate. The linear detection range of the electrode was determined to be between 0.01 mM and 0.1 mM (see Fig. 3-C and 3-D), obtaining a sensitivity of 439.8 ± 27.3 nA mM^{-1} ($R^2 = 0.99$). The estimated LOD has a value of 5 µM [25].

3.1.4. Stability and reproducibility

Reproducibility of the glucose biosensor PQQ-GDH@SWCNT-APPA-1.15 was investigated by detection of 10 mM glucose by cyclic voltammetry in 0.1 M PBS (pH = 7.2) in room atmosphere conditions for 3 different electrodes synthesized. As can be observed (see Fig. S8), electrochemical entrapment and electrochemical characterization in neutral conditions do not show important differences between the different electrodes prepared in the same manner. The relative standard deviation (RSD) of the current density variation at 0.4 V vs. Ag/AgCl (3 M KCl) for three different electrodes was 10%, demonstrating an adequate reproducibility of the electrocatalytic response of the bioelectrode towards glucose oxidation. Moreover, evaluation of the stability for the fabricated bioelectrodes by cyclic voltammograms (see Fig. S9) in absence and presence of 10 mM glucose shows that the stability after 24 h was 89%.

3.2. Immobilization of apo-GDH and subsequent in situ reconstitution

3.2.1. Electrochemical entrapment of apo-GDH on SWCNTs with 4-APPA

The potentiodynamic electrochemical entrapment of apo-GDH at different upper potential limits (see Fig. S10), shows that the voltammetric profiles obtained in presence of the apoenzyme are similar to those resulting in the electrochemical entrapment of the holoenzyme (Scheme 1, procedure 2). Similarly, to what was observed in procedure 2 the immobilization of the enzyme and electrochemical functionalization of the SWCNTs occur at the same time.

Fig. 4 shows the electrochemical characterization of the different electrodes in PBS electrolyte (pH = 7.2) obtained in presence of GDH at different upper potential limits. It can be observed in all cases that the oxidation of 4-APPA in presence of the apo-GDH generates stable

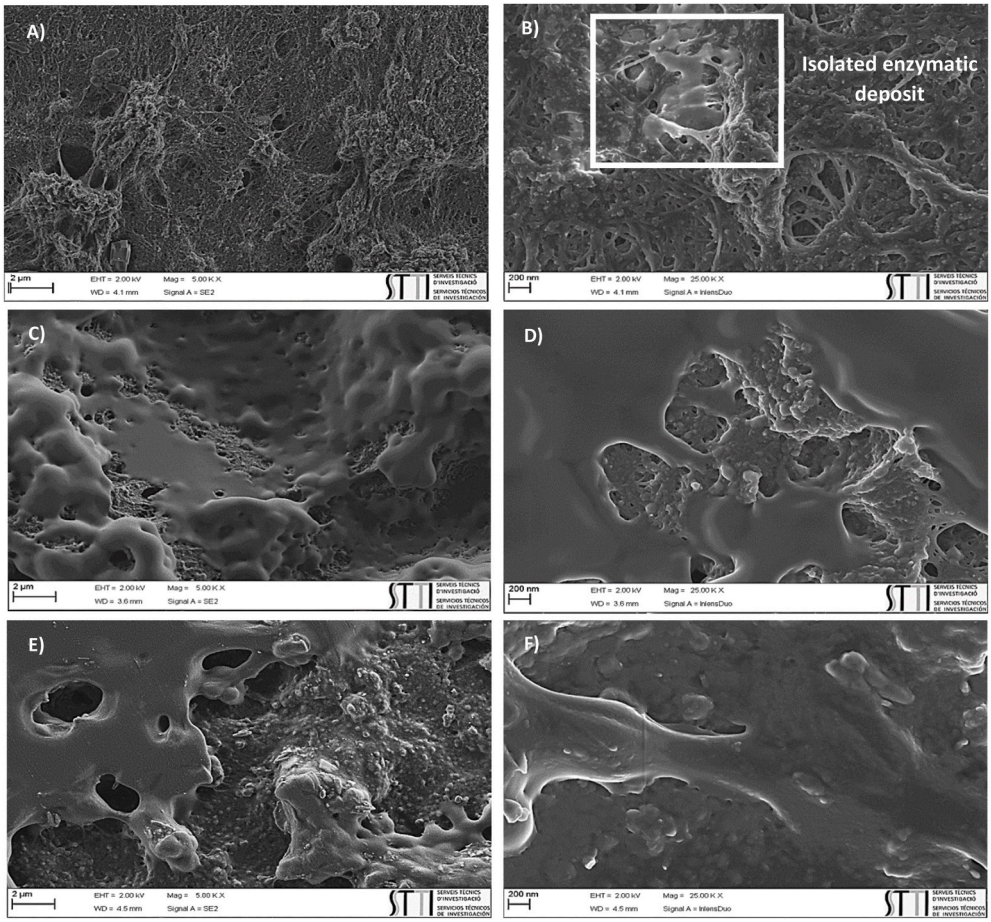

Fig. 2. FE-SEM micrographs of PQQ-GDH@SWCNT-APPA-X bioelectrodes synthesized at different upper potential limits: A-B) X = 0.75 V, C-D) X = 0.95 V and E-F) X = 1.15 V. Electrodes were modified under the following conditions: HEPES electrolyte + 5 mg mL^{-1} PQQ-GDH (pH = 5.0) at 50 mV s^{-1} for 50 cycles under Ar atmosphere.

electrochemical surface redox processes related with the species formed during SWCNTs functionalization, similar to the electrodes synthetized in absence of the apo-GDH (see Fig. S3). These redox processes are reversible, and their charge increases with the upper potential limit used during the functionalization step. Presence of apo-GDH decreases the double layer capacitance between −0.2 and 0 V in all cases that can be associated to the blockage of the SWCNTs surface by the enzyme. Also, an additional redox peak (A-A′) is observed in the GDH@SWCNT-APPA-X electrodes. The presence of the apo-GDH in the electrode tends to generate a more resistive behavior, observed in the slightly tilted voltammograms, but the main redox processes are clearly observed in the voltammograms.

Table 2 shows the XPS quantification for SWCNT-APPA-X electrodes. It can be observed that the amount of N is always higher than that of P and that the amount of N remains almost constant from an upper potential limit of 0.75 V, whereas the amount of P increases with the upper potential limit. This behavior is different to the observed during the functionalization in sulfuric acid [41], in which an increase of both N and P were observed. In HEPES electrolyte, the amount of both P and N is higher than the incorporated in acidic conditions, being significantly higher for P species. The observed behavior might be as a result of the less acidic conditions employed for the electrochemical entrapment, which do not promote the oxidation process of the phosphorus species and its desorption. Since additional oxidation of the electrolyte was observed at potentials more positive than 1.35 V vs. Ag/AgCl (3 M KCl) affecting the functionalization procedure, higher applied potentials were avoided (see Fig. S11).

In terms of the different contributions of N and P species, XPS N1s spectra (Fig. S12) show a peak at around 400.1 eV in all the potential limits studied. The main important contributions are related with the presence of neutral amines and imines species with binding energies at around 400.1 and 398.5 eV, respectively [41,48]. Furthermore, a small contribution associated with oxidized nitrogen species at binding energy around 401.5 eV are observed. Despite the polarization conditions used, no important changes are appreciated in the distribution of the species in the electrode.

In case of P2p spectra (Fig. S13), the two asymmetric doublets appear related with the C–P–O and C–O–P groups at 132.6 eV 133.3 eV, respectively, are observed. The position of these peaks is similar to the observed in the PQQ-GDH@SWCNT-APPA-X electrodes (Table 1). However, their distribution differs considerably with the electrode synthetized in presence of the enzyme, confirming that an interaction with the enzyme is established through the phosphorus groups, stabilizing the phosphonic species.

3.2.2. *Glucose oxidation on GDH/PQQ@SWCNT-APPA-X electrodes*

The modified electrodes have been used in the oxidation of glucose in order to evaluate their electrocatalytic activity. The GDH@SWCNT-APPA-X electrodes do not oxidize glucose (see Fig. S14), due to the absence of the cofactor (PQQ). Therefore, heterogeneous reconstitution of the immobilized apo-GDH enzyme, was carried out by drop-casting of the cofactor (PQQ) onto the GDH@SWCNT-APPA-X electrodes [49]. Fig. 5-A, 5-C and 5-E (dotted lines) show the cyclic voltammograms for the GDH/PQQ@ SWCNT-APPA-X electrodes. It can be clearly observed the appearance of the redox couple at around −0.11 V vs. Ag/AgCl (3 M KCl) assigned to the two-electron transfer of the PQQ [42,50],

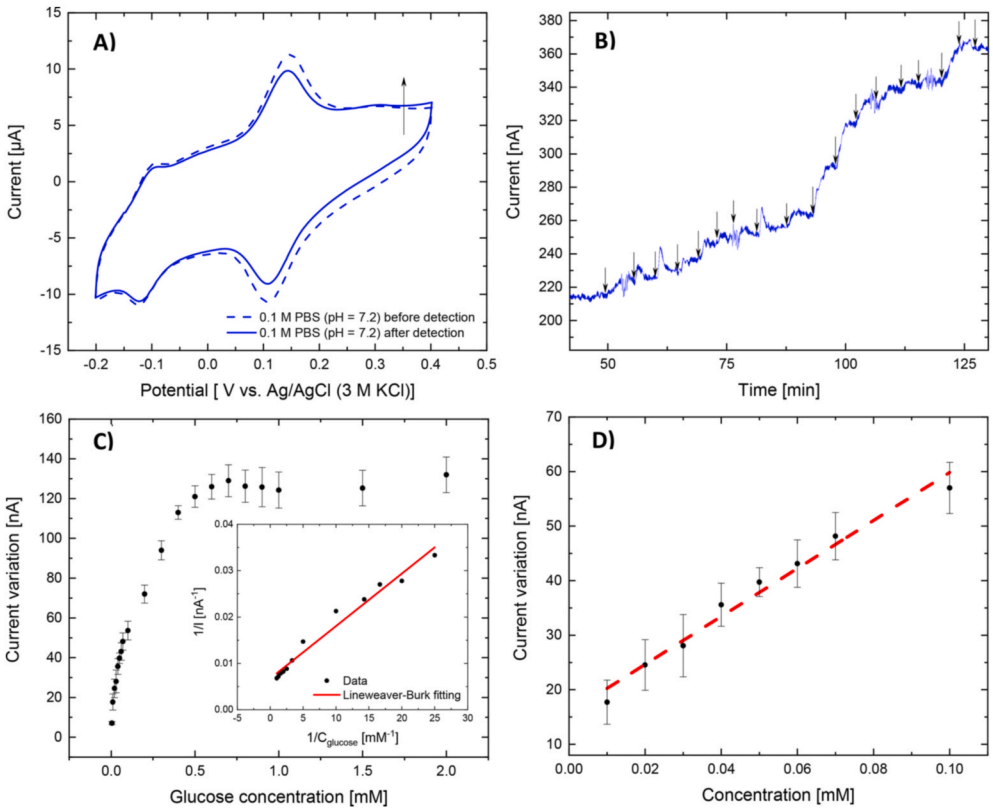

Fig. 3. A) Cyclic voltammograms of electrode GDH/PQQ@SWCNT-APPA-1.15 before and after the detection of glucose. B) Chronoamperometric response of GDH/PQQ@SWCNT-APPA-1.15 at 0.35 V vs. Ag/AgCl (3 M KCl) for different concentrations of glucose as indicated by the arrows: 0.005, 0.01, 0.02, 0.03, 0.04, 0.05, 0.06, 0.07, 0.1, 0.2, 0.3, 0.4, 0.5, 0.6, 0.7, 0.8, 0.9, 1, 1.5, 2 and 4 mM under room atmosphere conditions. C) Calibration curve. Inset: Lineweaver-Burk fitting for enzyme immobilization by Michaelis-Menten constant. D) Linear regression fitting.

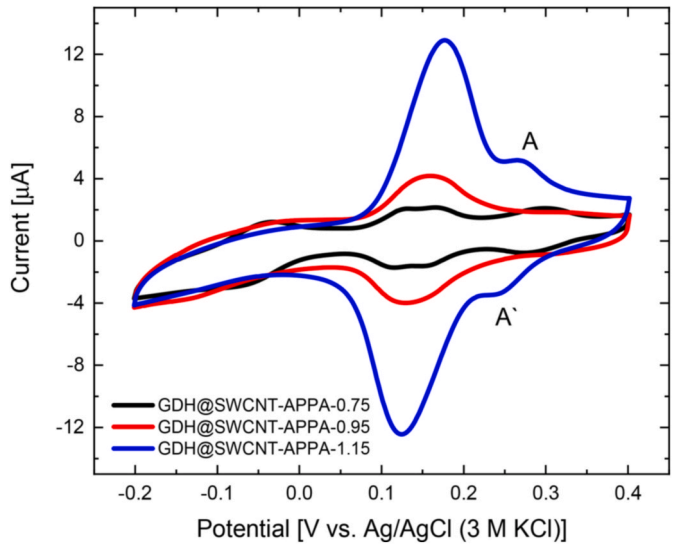

Fig. 4. Cyclic voltammograms of GDH@SWCNT-APPA-X electrodes. Electrochemical modification was carried out at different upper potential limits (0.75 V: black line, 0.95 V: red line and 1.15 V: blue line) at 50 mV s^{-1} for 50 cycles under Ar atmosphere. 0.1 M PBS (pH = 7.2) under room atmosphere conditions, 5 mV s^{-1}.

previously observed in PQQ-GDH@SWCNT-APPA-X electrodes.

In presence of glucose (Fig. 5-A, 5-C and 5-E, solid lines), the voltammetric charges of the redox functionalities decrease possibly as a consequence of leaching of immobilized enzyme promoted by a local pH change during the enzymatic reaction. The GDH/PQQ@SWCNT-APPA-1.15 electrode (Fig. 5-E) shows an oxidation current at more positive potentials, which can be associated to the oxidation of glucose in solution, producing an oxidation current of 2.3 μA at 0.4 V. Chronoamperometry response at 0.35 V (Fig. 5-B, 5-D and 5-F) demonstrates that when glucose is introduced in the solution in a concentration of 1.6 mM, all the electrodes present electrocatalytic activity towards glucose oxidation, confirming that the immobilized enzyme maintains its catalytic activity and the successful reconstitution of the enzyme with the PQQ cofactor.

The electrocatalytic activity is higher for the sample functionalized at 1.15 V. This can be explained considering either that the amount of immobilized enzyme is higher when the potential reaches a value of 1.15 V (the amount of functionalities in the SWCNT-APPA-1.15/GDH electrode is the highest, see Fig. 4) or that the chemical interaction between the enzyme and the functionalized SWCNT favors the most adequate orientation of the enzyme that improves the electron transfer with the electrode.

The PQQ surface concentration (Γ) was estimated from the reversible redox process at −0.11 V for all the three different potential evaluated for the GDH/PQQ@SWCNT-APPA-X electrodes, obtaining similar values at around (2.6 ± 0.7) x 10^{-10} mol cm^{-2}, which is considerably higher than values obtained in the PQQ-GDH@SWCNT-APPA-X electrodes. However, in this case, in addition to the PQQ present in the reconstituted enzyme the possible additional contribution of free-PQQ remaining adsorbed onto the electrode surface cannot be discarded. Interestingly, the electrocatalytic response towards glucose oxidation is considerably higher for the GDH/PQQ@SWCNT-APPA-1.15 electrode. Therefore, enhancement of the catalytic current must not be directly related with the concentration of the redox enzyme entrapped. In this sense, an increase in the electrocatalytic performance for enzyme-modified electrodes with an increased upper potential limit during electrochemical entrapment can be associated with favored interactions between the enzyme and the functional species on the SWCNTs during the electrochemical entrapment, considering that at the pH conditions used the acidic phosphorus groups are deprotonated, whereas the enzyme (with an isoelectric point of ~9.5) presents a net positive charge [35,51]. Then, P species can facilitate the electron transfer with the electrode, as

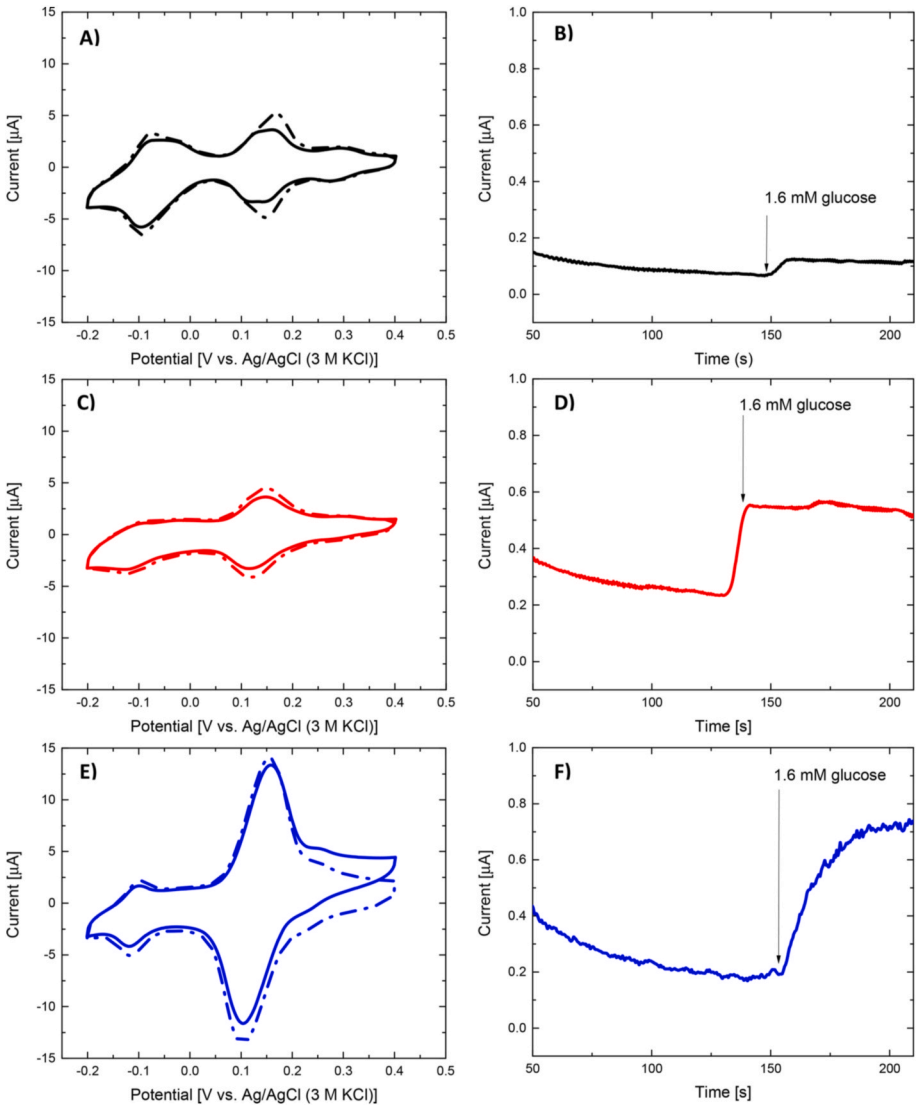

Fig. 5. Electrocatalytic performance of GDH/PQQ@SWCNT-APPA-X towards glucose oxidation synthesized at different upper potential limits (0.75 V (A, B), 0.95 V (C, D) and 1.15 V (E,F)). A, C and E) Cyclic voltammograms in absence (dotted line) and presence (solid line) of 4 mM glucose, in 0.1 M PBS (pH = 7.2) at room atmosphere conditions at 5 mV s^{-1}. B, D and F) Chronoamperometric response of GDH/PQQ@SWCNT-APPA-X in 0.1 M PBS (pH = 7.2) at room atmosphere conditions at a fixed potential of 0.35 V vs. Ag/AgCl (3 M KCl) before and after the addition of 1.6 mM glucose.

Table 2
Quantification of surface species by XPS and distribution of N and P contributions for SWCNT-APPA-X modified electrodes in HEPES electrolyte at different upper potential limits.

Upper potential limit [V vs. Ag/AgCl (3 M KCl)]	O (at %)	N (at %)	P (at %)	N/P[a]	% Neutral N species (398.5 and 400.1 eV)	% Oxidized nitrogen (401.5 eV)	% C–O–P (133.3 eV)	% C–P–O (132.6 eV)
Pristine	3.1	0.37	0.0	–	–	–	–	–
0.75	7.2	1.67	0.23	5.7	94	6	67	33
0.95	8.0	1.41	0.51	2.0	95	5	59	41
1.15	8.5	1.70	0.88	1.5	90	10	61	39

[a] The N content of the pristine SWCNT has been subtracted for the calculation.

has been observed with other negatively charged functional groups in polyaniline-based polymers and sulfonic-containing electrodes [52,53] and phosphorus-containing electrodes and other redox enzymes [54,55].

Fig. 6-A shows the chronoamperometry curves obtained at 0.35 V under stirring condition for glucose concentrations between 5.0 μM and 2.5 mM in 0.1 M PBS (pH = 7.2) for the GDH/PQQ@SWCNT-APPA-1.15 electrode. It can be observed an increase in the current after the addition of aliquots of glucose. Cyclic voltammograms before and after the detection of glucose in Fig. 6-B confirm the stability of the electrode. Fig. 6-C shows the calibration curve (variation of the current versus glucose concentration) which presents the Michaelis-Menten behavior. The limit of detection (LOD) was determined empirically, as the lowest concentration of glucose whose signal can be clearly distinguished from the background current, having a value of 5 μM. The linear fitting for the electrode is obtained in the concentration range between 0.01 mM and 0.1 mM, with a sensitivity of 981.7 ± 3.5 nA mM^{-1} ($R^2 = 0.99$) as can be observed in Fig. 6-D. Interestingly, the sensitivity in the same linear range obtained for the GDH/PQQ@SWCNT-APPA-1.15 electrode are two times higher than in the electrodes prepared with reconstituted holoenzyme. The obtained value of the apparent Michaelis-Menten constant (K_m^{app}) for the enzymatic biosensor was 0.39 mM (see inset in Fig. 6-C), which is lower to the values reported in solution (0.5–22 mM) [35,56], but higher than obtained for the PQQ-GDH@SWCNT-APPA-

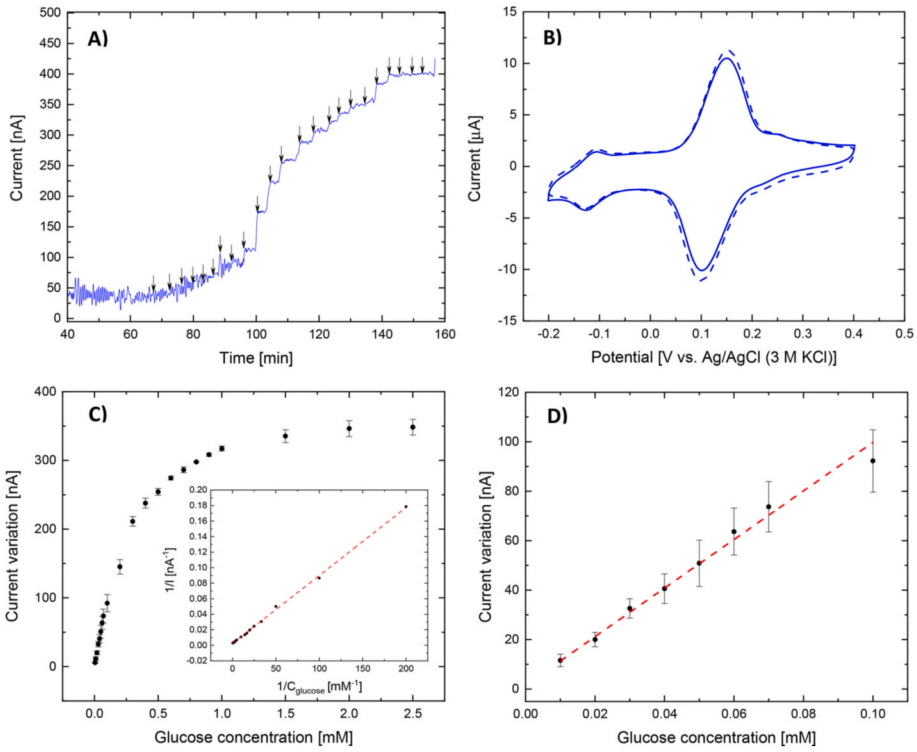

Fig. 6. A) Chronoamperometric curve for GDH/PQQ@ SWCNT-APPA-1.15 electrode at 0.35 V vs. Ag/AgCl (3 M KCl) for different concentrations of glucose as indicated by the arrows: 0.005, 0.01, 0.02, 0.03, 0.04, 0.05, 0.06, 0.07, 0.1, 0.2, 0.3, 0.4, 0.5, 0.6, 0.7, 0.8, 0.9, 1, 1.5, 2, 2.5, 3 and 4 mM under room atmosphere conditions. B) Cyclic voltammograms in buffer solution for the GDH/PQQ@SWCNT-APPA-1.15 electrode before (dash line) and after (solid line) the experiment shown in panel A. C) Current response as a function of glucose concentration. Inset: Lineweaver-Burk plot. D) Regression fitting for the linear range of the calibration plot.

1.15 electrode. Nevertheless, the low value of K_m^{app} obtained still suggests high affinity between the enzyme and the substrate.

The electrochemical behavior previously studied demonstrated the applicability of the electrochemical entrapment of apo-GDH employing anodic oxidation with 4-APPA, in presence of SWCNTs, and subsequent *in situ* reconstitution of the enzyme employing low concentrations of PQQ, for the fabrication of electrocatalytically active bioelectrodes for glucose oxidation.

3.2.3. *Comparison between electrochemical entrapment of enzyme and drop-casting method*

A comparison of the calibration curves for the electrodes prepared by electrochemical entrapment of the apo-GDH with 4-APPA at an upper potential of 1.15 V (GDH/PQQ@ SWCNT-APPA-1.15) and the and an electrode modified with 4-APPA at 1.15 V and subsequent immobilization of PQQ-GDH by drop-casting (SWCNT-APPA-1.15-PQQ-GDH$_{drop\text{-}casting}$ electrode) is presented in Fig. 7. The voltammogram of the electrode prepared by drop-casting and the chronoamperometry profile towards glucose oxidation for this electrode can be observed in Fig. S13.

The electrode synthesized by electrochemical entrapment of apo-GDH shows an important increase in sensitivity of up to 45% in the concentration range between 0.01 mM and 0.1 mM in comparison with an electrode prepared by a drop-casting procedure (see Fig. 7 and Table 3). Interestingly, in contrast with conventional drop-casting, a substantially lower amount of enzyme is employed during electrode synthesis. Moreover, the use of a smaller concentration of PQQ (40 μM) and the possibility to avoid centrifugation steps during apo-GDH reconstitution are important advantages of the proposed electrode fabrication procedure. A notorious enhancement in the sensitivity obtained for bioelectrodes prepared by electrochemical entrapment can be associated to an improved interconnection between enzyme and the electrode, in agreement with the lower K_m values observed. Possibly, favored electron-transfer kinetics of the enzyme by the phosphorus functionalities are directly related with the improvement in the electrocatalytic activity towards glucose oxidation [35,52].

A comparison of some important parameters obtained in this work

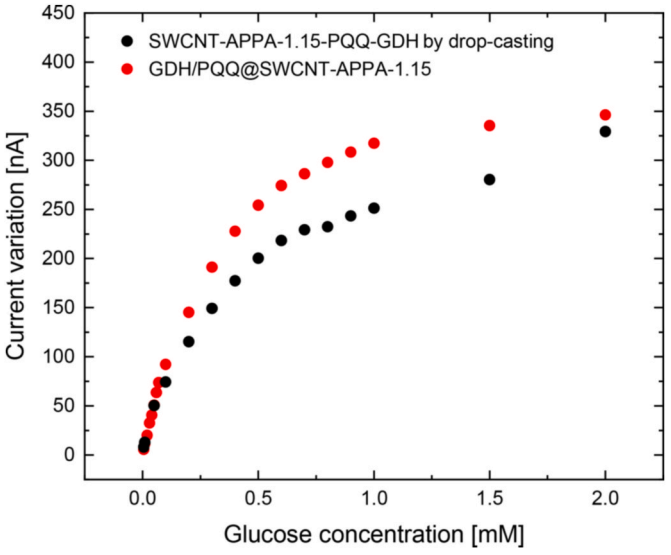

Fig. 7. Calibration curves for electrodes prepared by: i) electrochemical entrapment of apo-GDH with 4-APPA and subsequent reconstitution (GDH/PQQ@ SWCNT-APPA-1.15) in red dots and ii) SWCNT electrochemically modified with 4-APPA at 1.15 V and incubated with reconstituted PQQ-GDH by conventional manual deposition procedure (drop casting) in black dots (SWCNT-APPA-1.15-PQQ-GDH$_{drop\text{-}casting}$). (For interpretation of the references to colour in this figure legend, the reader is referred to the Web version of this article.)

with previous reports in literature of bioelectrodes for sensors and bioanodes applications employing PQQ-GDH is shown in Table S1. For most of the cases, the sensitivity attained with the reported modified electrodes is similar or superior in comparison with other bioelectrodes based on DET. However, in some cases performance might be higher as result of the effect of PQQ and formation of PQQ layers adsorbed that act as a redox mediator for electron transfer. Interestingly, most of the

Table 3
Analytical figures of merit for the quantification of glucose for electrodes prepared by electrochemical enzyme entrapment of apo- and holoenzyme, and a control electrode prepared by drop-casting.

Parameter	Bioelectrode		
	PQQ-GDH@ SWCNT-APPA-1.15	GDH/ PQQ@SWCNT-APPA-1.15	SWCNT-APPA-1.15-PQQ-$GDH_{drop\ casting}$
Coating of enzyme [mol cm^{-2}]	5.77 x 10^{-11}	2.57 x 10^{-10}	6.07 x10^{-10}
Sensitivity [nA mM^{-1}]	439.8 ± 27.3	981.7 ± 3.5	673.9 ± 12.9
R^2	0.99	0.99	0.98
Linear range (mM)	0.01–0.1	0.01–0.1	0.01–0.1
K_m^{app} (mM)	0.19	0.39	0.59

published platforms include multiple fabrication steps of the bioelectrode, such as functionalization of substrate, immobilization of the enzyme and crosslinking, in contrast with the methodology proposed in this research which is performed with lower number of steps. Additionally, electrochemical entrapment with 4-APPA guarantees that all the redox enzyme incorporated is in intimate contact with the electrode, favoring the DET mechanism and the immobilization of the enzyme.

4. Conclusions

The electrochemical entrapment of either apo-GDH or reconstituted PQQ-GDH during oxidation of *para*-aminophenyl phosphonic acid (4-APPA) provides a simple method for the immobilization of the enzyme onto the SWCNTs surface at the same time that functionalization of the SWCNTs with phosphorus and nitrogen groups also occurs. In the presence of the enzyme substrate a catalytic current is obtained for electrodes synthetized with the reconstituted holoenzyme, showing an efficient electrical contact between enzyme and electrode. Electrodes modified with apo-GDH only show electrocalytic activity towards glucose oxidation after incubation with PQQ, demonstrating that the enzyme is correctly entrapped, reconstituted with the redox cofactor and electrically wired with the electrode. These bioelectrodes show a high dependence of the electrocatalytic performance for glucose oxidation with the upper potential limit employed during electrochemical synthesis of the electrodes and concomitant enzyme immobilization. A higher performance is observed at higher upper potential limits used, in agreement with a higher degree of functionalization with P species. The improved catalytic activity towards glucose oxidation of the presented enzyme-modified electrodes in comparison with an electrode prepared by drop-casting, demonstrates an adequate interaction between the phosphorus groups incorporated in the material during the electrochemical co-deposition of films and the enzyme.

Regarding entrapment of apo-GDH and subsequent reconstitution, this procedure offers an interesting methodology which can overcome important limitations associated with enzyme reconstitution, such as tedious procedures for enzyme reconstitution and purification and the use of high concentrations of the redox cofactor for the reconstitution of enzyme in solution. In this sense, the methodology proposed offers a platform for simple enzymatic electrode preparation under mild synthesis conditions on nanostructured carbon-based materials. The methodology could be extended to other enzymes, in order to obtain improved direct electron transfer and enabling the manufacturing of electrodes in a single step for potential applications in bioelectrodes used in biofuel cells or for biosensing purposes.

Declaration of competing interest

The authors declare that they have no known competing financial interests or personal relationships that could have appeared to influence the work reported in this paper.

Acknowledgements

The authors would like to thank MICINN (PID2019-105923RB-I00) for the financial support. A.F.Q.J. gratefully acknowledges Generalitat Valenciana for the financial support through Santiago Grisolia grant (GRISOLIA/2016/084), to the University of Alicante for the support in the mobility program through the Escuela de Doctorado (EDUA).

Appendix A. Supplementary data

Supplementary data to this article can be found online at https://doi.org/10.1016/j.talanta.2021.122386.

Credit author statement

Andres Felipe Quintero-Jaime: Conceptualization, Methodology, Investigation, Writing – original draft. Felipe Conzuelo: Conceptualization, Methodology, Investigation. Diego Cazorla-Amorós: Conceptualization, Methodology, Supervision, Writing – review & editing, Funding acquisition. Emilia Morallón: Conceptualization, Methodology, Project administration, Supervision, Writing – review & editing, Funding acquisition.

References

[1] P. Bollella, E. Katz, Enzyme-based biosensors: tackling electron transfer issues, Sensors 20 (2020) 3517, https://doi.org/10.3390/s20123517.
[2] H.-L. Schmidt, W. Schuhmann, Reagentless oxidoreductase sensors, Biosens. Bioelectron. 11 (1996) 127–135, https://doi.org/10.1016/0956-5663(96)83720-1.
[3] A. Ruff, F. Conzuelo, W. Schuhmann, Bioelectrocatalysis as the basis for the design of enzyme-based biofuel cells and semi-artificial biophotoelectrodes, Nat. Catal. 3 (2020) 214–224, https://doi.org/10.1038/s41929-019-0381-9.
[4] R.J. Lopez, S. Babanova, K. Artyushkova, P. Atanassov, Surface modifications for enhanced enzyme immobilization and improved electron transfer of PQQ-dependent glucose dehydrogenase anodes, Bioelectrochemistry 105 (2015) 78–87, https://doi.org/10.1016/j.bioelechem.2015.05.010.
[5] W. Schuhmann, Amperometric enzyme biosensors based on optimised electron-transfer pathways and non-manual immobilisation procedures, Rev. Mol. Biotechnol. 82 (2002) 425–441, https://doi.org/10.1016/S1389-0352(01)00058-7.
[6] M. Albareda-Sirvent, A. Merkoçi, S. Alegret, Configurations used in the design of screen-printed enzymatic biosensors, A review, Sens. Actuat. B Chem. 69 (2000) 153–163, https://doi.org/10.1016/S0925-4005(00)00536-0.
[7] S. Ma, R. Ludwig, Direct electron transfer of enzymes facilitated by cytochromes, ChemElectroChem 6 (2019) 958–975, https://doi.org/10.1002/celc.201801256.
[8] M.C. Beilke, T.L. Klotzbach, B.L. Treu, D. Sokic-Lazic, J. Wildrick, E.R. Amend, L. M. Gebhart, R.L. Arechederra, M.N. Germain, M.J. Moehlenbrock, Sudhanshu, S. D. Minteer, in: T.S.B.T.-M.F.C. Zhao (Ed.), Chapter 5 - Enzymatic Biofuel Cells, Academic Press, Boston, 2009, pp. 179–241, https://doi.org/10.1016/B978-0-12-374713-6.00005-6.
[9] S.W. May, Applications of oxidoreductases, Curr. Opin. Biotechnol. 10 (1999) 370–375, https://doi.org/10.1016/S0958-1669(99)80067-6.
[10] P.N. Bartlett. Bioelectrochemistry: Fundamental, Experimental Techniques and Applications, first ed., Jhon Wiley & Sons, Ltd, Southampton, UK, 2008.
[11] S. López-Bernabeu, F. Huerta, E. Morallón, F. Montilla, Direct electron transfer to cytochrome c induced by a conducting polymer, J. Phys. Chem. C 121 (2017) 15870–15879, https://doi.org/10.1021/acs.jpcc.7b05204.
[12] K. Takeda, K. Igarashi, M. Yoshida, N. Nakamura, Discovery of a novel quinohemoprotein from a eukaryote and its application in electrochemical devices, Bioelectrochemistry 131 (2020) 107372, https://doi.org/10.1016/j.bioelechem.2019.107372.
[13] H. Teymourian, A. Barfidokht, J. Wang, Electrochemical glucose sensors in diabetes management: an updated review (2010–2020), Chem. Soc. Rev. 49 (2020) 7671–7709, https://doi.org/10.1039/D0CS00304B.
[14] A. Vilkanauskyte, T. Erichsen, L. Marcinkeviciene, V. Laurinavicius, W. Schuhmann, Reagentless biosensors based on co-entrapment of a soluble redox polymer and an enzyme within an electrochemically deposited polymer film, Biosens. Bioelectron. 17 (2002) 1025–1031, https://doi.org/10.1016/S0956-5663(02)00095-7.
[15] D.N. Tran, K.J. Balkus, Perspective of recent progress in immobilization of enzymes, ACS Catal. 1 (2011) 956–968, https://doi.org/10.1021/cs200124a.
[16] M. Shao, M. Nadeem Zafar, C. Sygmund, D.A. Guschin, R. Ludwig, C.K. Peterbauer, W. Schuhmann, L. Gorton, Mutual enhancement of the current density and the coulombic efficiency for a bioanode by entrapping bi-enzymes with Os-complex

modified electrodeposition paints, Biosens. Bioelectron. 40 (2013) 308–314, https://doi.org/10.1016/j.bios.2012.07.069.
[17] T. Lötzbeyer, W. Schuhmann, H.-L. Schmidt, Minizymes. A new strategy for the development of reagentless amperometric biosensors based on direct electron-transfer processes, Bioelectrochem. Bioenerg. 42 (1997) 1–6, https://doi.org/10.1016/S0302-4598(96)05187-2.
[18] S. Barwe, C. Andronescu, S. Pöller, W. Schuhmann, Codeposited poly(benzoxazine) and Os-complex modified polymethacrylate layers as immobilization matrix for glucose biosensors, Electroanalysis 27 (2015) 2158–2163, https://doi.org/10.1002/elan.201500131.
[19] A. Heller, Electrical connection of enzyme redox centers to electrodes, J. Phys. Chem. 96 (1992) 3579–3587, https://doi.org/10.1021/j100188a007.
[20] A. Ramanavicius, K. Habermüller, E. Csöregi, V. Laurinavicius, W. Schuhmann, Polypyrrole-entrapped quinohemoprotein alcohol dehydrogenase. Evidence for direct electron transfer via conducting-polymer chains, Anal. Chem. 71 (1999) 3581–3586, https://doi.org/10.1021/ac981201c.
[21] M. Abidi, S. López-Bernabeu, F. Huerta, F. Montilla, S. Besbes-Hentati, E. Morallón, Spectroelectrochemical study on the copolymerization of o-aminophenol and aminoterephthalic acid, Eur. Polym. J. 91 (2017) 386–395, https://doi.org/10.1016/J.EURPOLYMJ.2017.04.024.
[22] F. Wu, T. Huang, Y. Hu, X. Yang, Q. Xie, One-pot electrodeposition of a composite film of glucose oxidase, imidazolium alkoxysilane and chitosan on a reduced graphene oxide–Pt nanoparticle/Au electrode for biosensing, J. Electroanal. Chem. 781 (2016) 296–303, https://doi.org/10.1016/j.jelechem.2016.04.015.
[23] L. Betancor, H.R. Luckarift, Bioinspired enzyme encapsulation for biocatalysis, Trends Biotechnol. 26 (2008) 566–572, https://doi.org/10.1016/j.tibtech.2008.06.009.
[24] J. Liu, X. Wang, T. Wang, D. Li, F. Xi, J. Wang, E. Wang, Functionalization of monolithic and porous three-dimensional graphene by one-step chitosan electrodeposition for enzymatic biosensor, ACS Appl. Mater. Interfaces 6 (2014) 19997–20002, https://doi.org/10.1021/am505547f.
[25] A. Kausaite-Minkstimiene, V. Mazeiko, A. Ramanaviciene, A. Ramanavicius, Evaluation of amperometric glucose biosensors based on glucose oxidase encapsulated within enzymatically synthesized polyaniline and polypyrrole, Sensor. Actuator. B Chem. 158 (2011) 278–285, https://doi.org/10.1016/j.snb.2011.06.019.
[26] S. López-Bernabeu, A. Gamero-Quijano, F. Huerta, E. Morallón, F. Montilla, Enhancement of the direct electron transfer to encapsulated cytochrome c by electrochemical functionalization with a conducting polymer, J. Electroanal. Chem. 793 (2017) 34–40, https://doi.org/10.1016/j.jelechem.2016.12.044.
[27] C. Andronescu, S. Pöller, W. Schuhmann, Electrochemically induced deposition of poly(benzoxazine) precursors as immobilization matrix for enzymes, Electrochem. Commun. 41 (2014) 12–15, https://doi.org/10.1016/j.elecom.2014.01.015.
[28] Y. Tan, W. Deng, C. Chen, Q. Xie, L. Lei, Y. Li, Z. Fang, M. Ma, J. Chen, S. Yao, Immobilization of enzymes at high load/activity by aqueous electrodeposition of enzyme-tethered chitosan for highly sensitive amperometric biosensing, Biosens. Bioelectron. 25 (2010) 2644–2650, https://doi.org/10.1016/j.bios.2010.04.040.
[29] K. Habermüller, A. Ramanavicius, V. Laurinavicius, W. Schuhmann, An oxygen-insensitive reagentless glucose biosensor based on osmium-complex modified polypyrrole, Electroanalysis 12 (2000) 1383–1389, https://doi.org/10.1002/1521-4109(200011)12:17<1383::AID-ELAN1383>3.0.CO;2-0.
[30] B.J. Brownlee, M. Bahari, J.N. Harb, J.C. Claussen, B.D. Iverson, Electrochemical glucose sensors enhanced by methyl viologen and vertically aligned carbon nanotube channels, ACS Appl. Mater. Interfaces 10 (2018) 28351–28360, https://doi.org/10.1021/acsami.8b08997.
[31] M. Topçu Sulak, Ö. Gökdoğan, A. Gülce, H. Gülce, Amperometric glucose biosensor based on gold-deposited polyvinylferrocene film on Pt electrode, Biosens. Bioelectron. 21 (2006) 1719–1726, https://doi.org/10.1016/j.bios.2005.08.008.
[32] M. Ammam, J. Fransaer, Microbiofuel cell powered by glucose/O2 based on electrodeposition of enzyme, conducting polymer and redox mediators. Part II: influence of the electropolymerized monomer on the output power density and stability, Electrochim. Acta 121 (2014) 83–92, https://doi.org/10.1016/j.electacta.2013.12.129.
[33] A. Ramanavičius, A. Ramanavičienė, A. Malinauskas, Electrochemical sensors based on conducting polymer—polypyrrole, Electrochim. Acta 51 (2006) 6025–6037, https://doi.org/10.1016/j.electacta.2005.11.052.
[34] P.N. Barlett, J.M. Cooper, A review of the immobilization of enzymes in electropolymerized films, J. Electroanal. Chem. 362 (1993) 1–12, https://doi.org/10.1016/0022-0728(93)80001-X.
[35] G. Fusco, G. Göbel, R. Zanoni, E. Kornejew, G. Favero, F. Mazzei, F. Lisdat, Polymer-supported electron transfer of PQQ-dependent glucose dehydrogenase at carbon nanotubes modified by electropolymerized polythiophene copolymers, Electrochim. Acta 248 (2017) 64–74, https://doi.org/10.1016/j.electacta.2017.07.105.
[36] B.F.Y. Yon-Hin, C.R. Lowe, An investigation of 3-functionalized pyrrole-modified glucose oxidase for the covalent electropolymerization of enzyme films, J. Electroanal. Chem. 374 (1994) 167–172, https://doi.org/10.1016/0022-0728(94)03364-1.
[37] S. Cosnier, Biomolecule immobilization on electrode surfaces by entrapment or attachment to electrochemically polymerized films, A review, Biosens. Bioelectron. 14 (1999) 443–456, https://doi.org/10.1016/S0956-5663(99)00024-X.
[38] P. Pinyou, A. Ruff, S. Pöller, S. Ma, R. Ludwig, W. Schuhmann, Design of an Os complex-modified hydrogel with optimized redox potential for biosensors and biofuel cells, Chem. Eur J. 22 (2016) 5319–5326, https://doi.org/10.1002/chem.201504591.
[39] L. Marcinkevičienė, I. Bachmatova, R. Semėnaitė, R. Rudomanskis, G. Bražėnas, R. Meškiene, R. Meškys, Purification and characterisation of PQQ-dependent glucose dehydrogenase from Erwinia sp. 34-1, Biotechnol. Lett. 21 (1999) 187–192, https://doi.org/10.1023/A:1005499709935.
[40] Thermo Scientific XPS Simplified [Online], Thermo Scientific XPS, Phosphorus, 2020. Available at: https://xpssimplified.com/elements/phosphorus.php#appnotes. (Accessed 3 March 2018).
[41] A.F. Quintero-Jaime, D. Cazorla-Amorós, E. Morallón, Electrochemical functionalization of single wall carbon nanotubes with phosphorus and nitrogen species, Electrochim. Acta 340 (2020) 135935, https://doi.org/10.1016/j.electacta.2020.135935.
[42] E. Katz, D.D. Schlereth, H.-L. Schmidt, Electrochemical study of pyrroloquinoline quinone covalently immobilized as a monolayer onto a cystamine-modified gold electrode, J. Electroanal. Chem. 367 (1994) 59–70, https://doi.org/10.1016/0022-0728(93)03010-M.
[43] D. Sarauli, C. Xu, B. Dietzel, B. Schulz, F. Lisdat, Differently substituted sulfonated polyanilines: the role of polymer compositions in electron transfer with pyrroloquinoline quinone-dependent glucose dehydrogenase, Acta Biomater. 9 (2013) 8290–8298, https://doi.org/10.1016/j.actbio.2013.06.008.
[44] J.S. Stevens, A.C. de Luca, M. Pelendritis, G. Terenghi, S. Downes, S.L. M. Schroeder, Quantitative analysis of complex amino acids and RGD peptides by X-ray photoelectron spectroscopy (XPS), Surf. Interface Anal. 45 (2013) 1238–1246, https://doi.org/10.1002/sia.5261.
[45] F. Quesada-Plata, R. Ruiz-Rosas, E. Morallón, D. Cazorla-Amorós, Activated carbons prepared through H3PO4-assisted hydrothermal carbonisation from biomass wastes: porous texture and electrochemical performance, Chempluschem 81 (2016) 1349–1359, https://doi.org/10.1002/cplu.201600412.
[46] C. Tanne, G. Göbel, F. Lisdat, Development of a (PQQ)-GDH-anode based on MWCNT-modified gold and its application in a glucose/O_2-biofuel cell, Biosens. Bioelectron. 26 (2010) 530–535, https://doi.org/10.1016/j.bios.2010.07.052.
[47] D. Sarauli, M. Riedel, C. Wettstein, R. Hahn, K. Stiba, U. Wollenberger, S. Leimkühler, P. Schmuki, F. Lisdat, Semimetallic TiO_2 nanotubes: new interfaces for bioelectrochemical enzymatic catalysis, J. Mater. Chem. 22 (2012) 4615–4618, https://doi.org/10.1039/C2JM16427B.
[48] J. Quílez-Bermejo, A. Ghisolfi, D. Grau-Marín, E. San-Fabián, E. Morallón, D. Cazorla-Amorós, Post-synthetic efficient functionalization of polyaniline with phosphorus-containing groups. Effect of phosphorus on electrochemical properties, Eur. Polym. J. 119 (2019) 272–280, https://doi.org/10.1016/j.eurpolymj.2019.07.048.
[49] L. Zhang, R. Miranda-Castro, C. Stines-Chaumeil, N. Mano, G. Xu, F. Mavré, B. Limoges, Heterogeneous reconstitution of the PQQ-dependent glucose dehydrogenase immobilized on an electrode: a sensitive strategy for PQQ detection down to picomolar levels, Anal. Chem. 86 (2014) 2257–2267, https://doi.org/10.1021/ac500142e.
[50] M. Zayats, E. Katz, R. Baron, I. Willner, Reconstitution of apo-glucose dehydrogenase on pyrroloquinoline quinone-functionalized Au nanoparticles yields an electrically contacted biocatalyst, J. Am. Chem. Soc. 127 (2005) 12400–12406, https://doi.org/10.1021/ja052841h.
[51] Y.-P. Kim, S.J. Park, D. Lee, H.-S. Kim, Electrochemical glucose biosensor by electrostatic binding of PQQ-glucose dehydrogenase onto self-assembled monolayers on gold, J. Appl. Electrochem. 42 (2012) 383–390, https://doi.org/10.1007/s10800-012-0409-1.
[52] G. Göbel, I.W. Schubart, V. Scherbahn, F. Lisdat, Direct electron transfer of PQQ-glucose dehydrogenase at modified carbon nanotubes electrodes, Electrochem. Commun. 13 (2011) 1240–1243, https://doi.org/10.1016/j.elecom.2011.08.034.
[53] D. Sarauli, C. Xu, B. Dietzel, B. Schulz, F. Lisdat, A multilayered sulfonated polyaniline network with entrapped pyrroloquinoline quinone-dependent glucose dehydrogenase: tunable direct bioelectrocatalysis, J. Mater. Chem. B. 2 (2014) 3196–3203, https://doi.org/10.1039/C4TB00336E.
[54] K. Yasutaka, Y. Takato, K. Takashi, M. Kohsuke, Y. Hiromi, Enhancement in adsorption and catalytic activity of enzymes immobilized on phosphorus- and calcium-modified MCM-41, J. Phys. Chem. B 115 (2011) 10335–10345, https://doi.org/10.1021/jp203632g.
[55] Y. Chen, X.-J. Yang, L.-R. Guo, J. Li, X.-H. Xia, L.-M. Zheng, Direct electrochemistry and electrocatalysis of hemoglobin at three-dimensional gold film electrode modified with self-assembled monolayers of 3-mercaptopropylphosphonic acid, Anal. Chim. Acta 644 (2009) 83–89, https://doi.org/10.1016/J.ACA.2009.04.027.
[56] F. Lisdat, PQQ-GDH – structure, function and application in bioelectrochemistry, Bioelectrochemistry 134 (2020) 107496, https://doi.org/10.1016/j.bioelechem.2020.107496.